ChemSusChem

Research Article
doi.org/10.1002/cssc.202400962

Chemistry Europe
European Chemical Societies Publishing

www.chemsuschem.org

VIP *Very Important Paper*

Model-Assisted Optimization of Xylose, Arabinose, Glucose, Mannose, Galactose and Real Hemicellulose Streams Dehydration To (Hydroxymethyl)Furfural and Levulinic Acid

Ana Jakob,[a, b] Blaž Likozar,[a] and Miha Grilc*[a, b]

Conversion of hemicellulose streams and the constituent monosaccharides, xylose, arabinose, glucose, mannose, and galactose, was conducted to produce value-added chemicals, including furfural, hydroxymethylfurfural (HMF), levulinic acid and anhydrosugars. The study aimed at developing a kinetic model relevant for direct post-Organosolv hemicellulose conversion. Monosaccharides served as a tool to in detail describe the kinetic behavior and segregate contribution of hydrothermal decomposition and acid catalyzed dehydration at the temperature range of 120–190 °C. Catalyst free aqueous media demonstrated enhanced formation of furanics, while elevated temperatures led to significant saccharide isomerization. The introduction of sulfuric and formic acids maximized furfural yield and significantly reduced HMF concentration by facilitating its rehydration into levulinic acid (46 mol%). Formic acid additionally substantially enhanced formation of anhydrosaccharides. An excellent correlation between modeled and experimental data enabled process optimization to maximize furanic yield in two distinct hemicellulose streams. Sulfuric acid-containing hemicellulose stream achieved the highest furfural yield after 30 minutes at 238 °C, primarily due to the high Ea for pentose dehydration (150–160 kJ mol^{-1}). Contrarily, formic acid-containing hemicellulose stream enabled maximal furfural yield at more moderate temperature and extended reaction time due to its lower Ea for the same reaction step (115–125 kJ mol^{-1}).

Introduction

Despite continuous efforts and persistent research, biomass conversion remains challenging due to the intricate nature and variability of lignocellulosic feedstocks.[1,2] However, lignocellulosic biomass, composed of hemicellulose, cellulose, and lignin, offers immense potential as a renewable source for bio-based platform chemicals.[3–5] While cellulose and lignin have been extensively studied, hemicellulose often remains underutilized.[6,7]

Hemicellulose is a polysaccharide, rich in pentoses like xylose and arabinose, although hexoses such as glucose, galactose and mannose may also be present.[8] As such, it can be hydrolyzed to monosaccharides that can be efficiently valorized towards different bio-based chemicals such as furanics (hydroxymethylfurfural and furfural) and levulinic acid by acid-catalyzed dehydration.[9–11]

Acid catalyzed saccharide dehydration traditionally relies on the use of homogeneous acid catalysts such as different mineral and organic acids.[12] Thus far, xylose[13] and glucose[14–17] are the most frequently studied model compounds to investigate pentose and hexose conversion to furanics and/or levulinic acid.[18] Besides glucose and xylose, other sugars commonly present in the hemicellulose fraction can contribute to the complexity of the studied system.[19] Consequently, kinetic studies of individual sugars can provide crucial information on identifying rate-determining steps and key intermediates.[9,20,21] Although galactose, mannose and arabinose are typically not the subject of most studies or are sometimes neglected due to their low concentrations in most hemicellulose streams, they can significantly differ in reactivity and reaction kinetics compared to xylose and glucose. For example, Garrett et al. investigated the underlying mechanisms of ketose and aldose dehydration to furanics and demonstrated a significant difference in reactivity due to the steric orientation of specific OH-groups.[22]

Additionally, identifying key kinetic parameters for acid-catalyzed dehydration of individual hemicellulose-derived monosaccharides enables the determination of suitable process conditions for obtaining maximum yields of desired final products, which can be directly transferred to real hemicellulose feedstocks. Thus far, only a limited number of studies report semi-mechanistic kinetic models for the conversion of real (hemi)cellulose streams under hydrothermal and acidic conditions.[23,24] Dussan et al. is one of few studies reporting the conversion of multiple hemicellulose derived saccharides, namely arabinose, xylose, and glucose in formic acid that includes transferability of calculated kinetic parameters to industrially relevant hemicellulose liquors.[25] The authors pri-

[a] *Department of Catalysis and Chemical Reaction Engineering, National Institute of Chemistry, Ljubljana, Slovenia*
[b] *University of Nova Gorica, Nova Gorica, Slovenia*

***Correspondence:** Dr. Miha Grilc, Department of Catalysis and Chemical Reaction Engineering, National Institute of Chemistry, Hajdrihova 19, Ljubljana 1000, Slovenia.*
Email: miha.grilc@ki.si

Supporting Information for this article is available on the WWW under https://doi.org/10.1002/cssc.202400962

marily focused on formic acid-catalyzed dehydration, without addressing potential degradation in the absence of a catalyst or provided a comparison between other homogeneous acid catalysts.

Existing kinetic studies utilize different modeling approaches such as power-law, first-order, or pseudo-first order to describe the kinetics of sugar dehydration in acidic media.[9,26,27] However, the influence regarding thermal instability of sugars in the reaction medium without a catalyst is rarely considered.[28] Studying the kinetics of sugar conversion in the absence of a catalyst can provide insights into the underlying mechanisms to distinguish between the catalytic activity and thermal/solvent effects, allowing predictive kinetic models.[11,29]

This study investigates the kinetics of five relevant saccharides in three different reaction media: hot liquid water (HLW), formic, and sulfuric acid, in the temperature range of 120–190 °C. Therefore, the objective is to thoroughly describe sugar dehydration by separating acid-catalyzed reactions from their thermal decomposition in HLW to more accurately identify relevant kinetic parameters such as reaction rate constants and activation energies. Furthermore, this work also follows the formation of anhydrosaccharides, which are often neglected in most other studies, to elucidate more mechanistic details during sugar dehydration.[30–32]

The aim of this study is to bridge the gap between the kinetics of individual sugars and real hemicellulose streams/liquors. Considering industrial relevant hemicellulose streams, specific monosaccharides (xylose, arabinose, glucose, galactose, and mannose) and reaction media (H_2SO_4 and formic acid) relevant to Organosolv processes (Organosolv process from FhG CBP and Formosolv-like process) were selected for this work. During the Organosolv process, biomass is treated at elevated temperatures (140–220 °C) in the presence of a homogeneous acid and a fractionation media containing water and an organic solvent, which offers exceptional process flexibility and efficient isolation of all main components of lignocellulosic biomass.[33,34] Pre-treatment processes like Organosolv result in hemicellulose streams containing multiple monosaccharides and homogeneous acids (e.g., sulfuric, formic acid) that can inherently act as catalysts.[35] Therefore, it is crucial to consider prior process steps and the actual composition of industrial available hemicellulose to obtain kinetic data relevant for more effective valorization of real hemicellulose stream.

The combined effect of multiple sugars present in hemicellulose liquor was validated using real hemicellulose streams. The comprehensive kinetic model developed in this study enabled the optimization of process parameters such as time and temperature to obtain the maximum yield of furfural utilizing two real hemicellulose streams. Furthermore, this work is one of the few studies that utilizes the complex kinetic behavior of individual sugars in several reaction media to effectively predict the optimization of furfural during the acid-catalyzed dehydration of two distinct, industrially relevant, hemicellulose mixtures.

Experimental

Materials

Dehydration reactions were performed using various pento- and hexoses D-(+)-xylose (SAFC®, ≥99%), L-(+)-arabinose (Sigma Aldrich, ≥99%) D-(+)-glucose (Merck), D-(+)-mannose, (Sigma Aldrich, ≥99%) and D-(+)-galactose (Sigma Aldrich, ≥99%) as substrates and as quantification standards. The reaction products were quantified using external standards such as furfural (Sigma Aldrich, 99%), hydroxymethylfurfural (Sigma Aldrich, 99%), 1,6-anhydro-D-galactofuranose (Synthose, 98%), 1,6-anhydro-D-galactopyranose (Biosinth, 98%), 1,6-anhydro-D-glucopyranose (Synthose, 98%), 1,6-anhydro-D-glucopyranose (TCI, ≥99%), 1,6-anhydro-D-mannopyranose (Biosinth), ribulose (Sigma Aldrich, ≥90%), levulinic acid (Sigma Aldrich, 98%), and formic acid (Sigma Aldrich, ≥98%). The dehydration reactions were carried out in different acidic aqueous media (miliq) using organic and mineral acids, namely formic (Sigma Aldrich, ≥98%) and sulfuric acids (Honeywell, 95–97 wt.% H_2SO_4).

Analytical Methods

The reaction substrates, namely various monosaccharides (arabinose, xylose, glucose, galactose, and mannose) and products such as furans (furfural and HMF) and organic acids (levulinic acid and formic acid) were identified and quantified using ultrahigh-pressure liquid chromatography (UHPLC-DAD /RI, Ultimate 3000, Thermo Scientific). The analytical method used is described in detail in our previous study.[18] In addition to Rezex Monosaccharide H^+ column, Rezex Monosaccharide Ca^{2+} column was utilized to quantify the isomerization (keto- and anhydrosugars) products. Due to similar responses of particular monosaccharides, lyxose was selected as reference compound for determining xylulose concentration.[18,36] A similar method was applied for the determination of tagatose concentrations, where galactose was used as the reference compound.[36] Additionally, for the hexose dehydration reaction carried out in high formic acid concentration, it was assumed that the formation of formic acid was stoichiometrically equal to the formation of levulinic acid.

Saccharide Conversion

Low temperature (120–140 °C) dehydration reactions were performed in 20-mL rolled-rim/crimphals glass vials of N20 to avoid possible corrosion. The vials were sealed with pressure-relief caps, placed in an oven and stirred individually with magnetic stir bars. The oven was set to the desired temperature (120–140 °C), and the temperature in the vials was controlled by an additional external thermocouple. The reaction solution was prepared by weighing out an exact amount of each sugar and acid catalyst in a volumetric flask. The solution was then transferred to 5 vials, each containing 10 ml of reaction solution. To study the kinetics of the saccharide dehydration reaction, each vial was removed from the oven after a certain time and quenched in water to obtain the concentration profiles of the reactants and reaction products at different temperatures and catalyst concentrations. High temperature (160–190 °C) dehydration reactions were carried out in 75 mL Hastelloy Parr reactors, equipped with sampling tube. The stir speed was set to 800 rpm. No mass transfer limitations were observed above 200 rpm, as presented in Supplementary Information, Figure 3. Reactions were performed in a manner where 50 mL of acidic solution with 1 wt.% of saccharide (arabinose/xylose/glucose/mannose/galactose) was placed into the reactor. In order to study the concentration of reactants and products as a function of time, 6

samples were taken at specific time intervals. The total reaction time including the heating ramp-up time of 5 °C/min was 5 hours. The samples were later filtered using 0.2 μm PET filters and analyzed offline by ultra-high-performance liquid chromatography (UHPLC). The concentration of H^+ ions was calculated using the dissociation constant and activity coefficient at a given reaction temperature.

The Eq. 1 and Eq. 2 were later used to calculate the saccharide conversion and product yield.

$$X_j(t) = \frac{c_{j(0)} - c_{j(t)}}{c_{j(0)}} \times 100 \quad (1)$$

$$Y_i(t) = \frac{c_{i(t)}}{c_{\text{reactant}(0)}} \times 100 \quad (2)$$

Where Equation 1 denotes the conversion *(Xj)* of component j (arabinose, xylose, mannose, glucose, or galactose), while $c_{j(0)}$ and $c_{j(t)}$ refer to the initial concentration of saccharide j and the concentration of each compound at the specific sampling time. Equation 2 refers to the calculation of the molar yield of product i, where $c_{i(t)}$ is its concentration at the given sampling time and reactant *(0)* is the initial concentration of the selected saccharide. Repeatability of the conducted experiments was estimated by conducting triplicates of glucose dehydration catalyzed by 1 g L^{-1} of H_2SO_4 and is demonstrated in Supporting Information, Figure S2.

Biomass Fractionation

For the final optimization of hemicellulose conversion, two different Organosolv-derived hemicellulose feedstocks were tested. The first hemicellulose stream was provided by Fraunhofer CBP Leuna, using beech wood as feedstock and ethanol-based Organosolv as fractionation process, later on referred to as *H.S.* Due to the presence of the oligomeric saccharides, an additional hydrolysis step was required. This included processing of the stream at 160 °C for 1 hour, including the ramp-up time in a 75 mL Hastelloy Parr reactor. The second hemicellulose stream (*H.F.*) was obtained by fractionation of beech wood sawdust (sieved to a particle size 710 μm) using 90 wt.% formic acid as fractionation solvent. 1.5 g of sawdust were placed in to a pressure tube and heated to boiling (105 °C) using an oil bath. The mixture was stirred magnetically. After 90 minutes, the slurry was filtered off and washed. The primary filtrate was later diluted with 3 parts water to precipitate the lignin fraction.[37–39] The liquid hemicellulose fraction was filtered off and later used for conversion to furanics. The concentration of monosaccharides in both hemicellulose streams subjected to dehydration reactions was measured by HPLC-method described above. To analyze the acid soluble and insoluble lignin, a hydrolysis was performed according to the NREL protocol,[40,41] in which the mixture was heated at 121 °C for 60 minutes in the presence of 4 wt.% of sulfuric acid. The slurry was then filtered off using filtering crucibles. The acid soluble lignin was measured by spectrophotometer UV–VIS. The filter cake represented the acid-insoluble lignin and was washed with miliq water and dried overnight at 105 °C.

Analysis of the diluted aqueous hemicellulose solution provided the detailed composition of the stream, which is described in Table 1. Various pentoses, including xylose and arabinose, as well as hexoses like galactose, mannose, and glucose, were quantified in the provided stream hemicellulose stream. In addition, the content of acid-soluble and insoluble lignin content was determined. Based on the compositional analysis, the hemicellulose sample obtained with ethanol as fractionation solvent resulted in diluted aqueous solution of glucose, xylose, arabinose, mannose and galactose with a pH of 2.1 and a dry matter content of 3.5 wt.%. In contrast, the hemicellulose fraction obtained after fractionation of beech wood with formic acid (30 wt./vol.%) resulted in similar composition of monosaccharides, while the total saccharide content appeared to be significantly lower.

Table 1. Composition of real hemicellulose stream a) Ethanol organosolv - FhG stream, after solvent recovery and b) fomic acid organosolv fractionation of beechwood.

Starting feedstock	H.S. Concentration [mmol L^{-1}]	H.F. Concentration [mmol L^{-1}]
Glucose	8.7	0.9
Xylose	111	26
Galactose/Mannose	9.6	n.a.
Arabinose	6.7	3.9
Acid insoluble lignin	< 0.5 wt.%	n.a.
Acid soluble lignin	2.74×10^3	n.a.

Development of Reaction Network and Kinetic Model

The kinetic model was developed for each individual saccharide based on the quantified liquid products based on already established and well-studied mechanisms of saccharide dehydration.[14,16,42,43] The reaction network for acid catalyzed dehydration of pentoses (xylose and arabinose) and hexoses (mannose, glucose, galactose) is presented in Figure 1 and Figure 4.

As presented, all reactions followed first order reaction kinetics. As saccharide degradation can proceed at elevated temperatures in the absence of a catalyst, the reaction rate depends only on the concentration of the specific reactant and the reaction rate constant, as shown in equations 5. While in acid-catalyzed reactions, the reaction rate depends on the concentration of the reactant, the reaction rate constant and the concentration of H^+ ions. The concentration of H^+ ions at the specific reaction temperature was calculated by the following equation 3 and 4 based on the equilibrium constant and temperature dependent function of sulfuric and formic acid dissociation.[17,44–46]

$$pK_A(\text{HCOOH}) = -57.528 + 2773.9\frac{1}{T} - 9.1232 \times ln(T) \quad (3)$$

$$pK_A\left(HSO_4^-\right) = T \times 0.0152 + 2.363 \quad (4)$$

$$r_i^{\text{homo}} = k_i\, C_j \quad (5)$$

$$r_i^{acid} = k_a\, C_j \quad (6)$$

$$k_a = k_i C_{H^+} \quad (6\,a)$$

$$\frac{dC_j^L}{dt} = \sum \pm r_i^{\text{homo}} + \sum \pm r_i^{acid} \quad (6\,b)$$

For the acid catalyzed reaction, the k_a represents the apparent reaction rate constant, that is, defined as a product of the intrinsic reaction rate constant and concentration of H^+ ions, as depicted in the Equation 6a due to linear dependency of H^+ and k_a.[17] Molar balances were expressed as a system of ordinary differential equations (**6b**). These equations were later numerically solved in

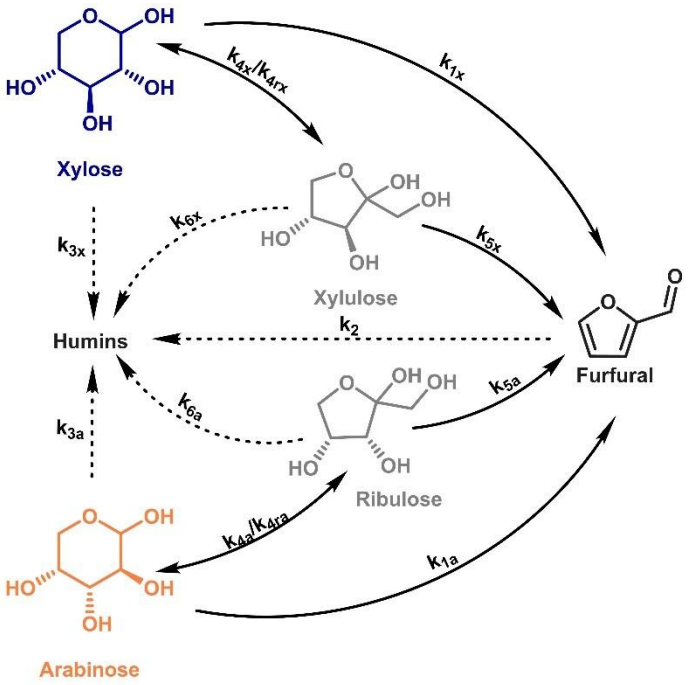

Figure 1. Proposed reaction network of pentose (arabinose and xylose) conversion.

Matlab 2018 utilizing the Runge–Kutta 2–3 method. The influence of temperature on the reaction rate constants was considered by incorporating the Arrhenius law, as presented in Eq. 7.

$$f\left(k_{i-j},\ Ea_{i-j}\right) = \sum_{exp=1}^{EXP}\sum_{j=1}^{J}\left(C^{L}_{j\,exp} - C^{L}_{j\,mod}\left(k_{i-j}, Ea_{i-j}\right)\right)^{2} \quad (8)$$

The Nelder–Mead method, demonstrated in Equation 8, was employed as a regression method for the minimization of the objective function.

Results and Discussion

Mechanism of Pentose Dehydration

Pentoses such as xylose and arabinose are known to be dehydrated to furfural through three consecutive water removal steps.[47] Although existing mechanistic studies generally support the theory of acyclic dehydration pathway through either β-elimination or 1,2-hydride shift, there remains no clear consensus on the key intermediates formed during pentose dehydration reactions.[48,49] Nevertheless, the precise mechanisms governing pentose dehydration and the formation of specific intermediates remains a subject of ongoing debate in the current literature.[12] Danon et al., suggested the coexistence of both of these proposed mechanisms is more likely, with their distinct prevalence depending largely on the specific reaction conditions employed.[9] To better understand the dehydration of complex hemicellulose mixtures, the kinetics of arabinose and xylose conversion were studied individually. A reaction network has been developed based on existing literature and the quantification of all detectable liquid products.[28,50,51] The reaction scheme shown in Figure 1 comprises of the following reaction steps: k1 describes the direct dehydration of pentose (arabinose/xylose) to furfural; k2, k3, k6 demonstrate the degradation of furfural, arabinose/xylose and their respective isomer to humins, respectively; while k4 and k4r denote reversible isomerization reactions and k5 represents direct dehydration of the respective isomer to furfural.[43,50–52]

Dehydration of Pentoses in Hot Liquid Water

Acknowledging the (hydro)-thermal instability of the investigated monosaccharides, dehydration reactions within this study were primarily carried out in aqueous media without the addition of a catalyst.[53] While various mechanisms can be found in the literature explaining this phenomenon, one of the most common explanations for the substantial amount of furanics produced in so-called high-temperature liquid water (HLW, $>160\,^{\circ}C$) is the increased concentration of H^{+} and OH^{-} ions.[18,54,55] However, it is important to consider that the concentration of these ions remains relatively low, consequentially there is an ongoing debate regarding their relative contribution to the acid-catalyzed dehydration of saccharides.[56–58]

To assess the kinetics of pentose conversion in catalyst-free hot liquid water, aqueous solutions of arabinose was subjected to hydrothermal treatment within the temperature range of 160–190 °C, as demonstrated in Figure 2. As shown in Figure S6 within the Supporting information, the conversion of arabinose,

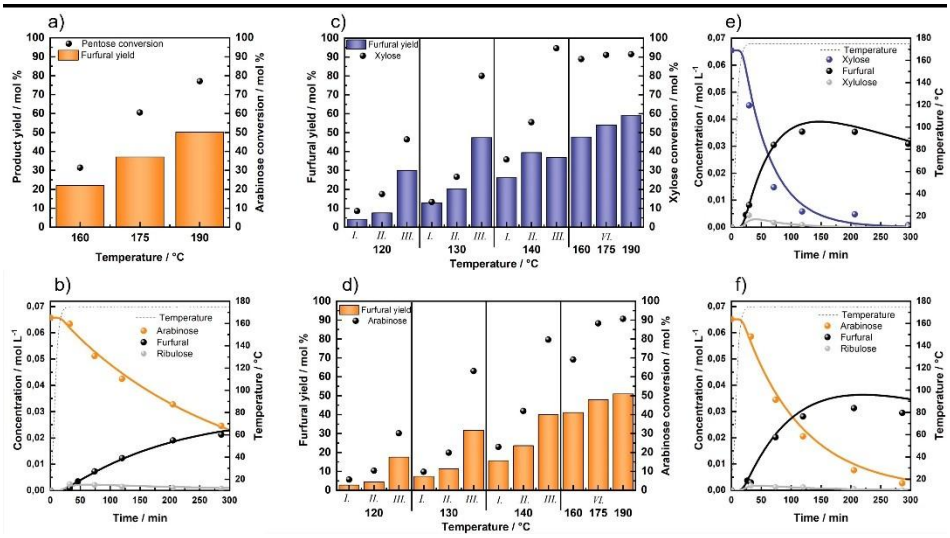

Figure 2. a) Maximal furfural yield and arabinose conversion at different temperatures in catalyst free HLW and b) product distribution as a function of the time for arabinose dehydration reaction in HLW at 175 °C. Maximal furfural yield and pentose conversion at different temperatures c) xylose d) arabinose conversion catalysed by sulfuric acid, where *I., II., III., IV.*, correspond to acid concentrations of 5, 10, 50 and 1 g/L. Product distribution as a function of the time for e) xylose and f) arabinose dehydration reaction catalysed by sulfuric acid (1 g/L) at 175 °C.

furfural yield and isomerization products exhibited a pronounced temperature dependence. As the temperature increased, both the yield and conversion significantly improved, analogous to what was reported by Jing et al. and Chen et al.[55,59]

Arabinose dehydration resulted in the highest furfural yield (43 mol%) at the temperature of 190 °C, which was comparable to xylose dehydration under the same conditions as reported in previous study.[18] Elaborating on the study of xylose conversion in HLW, a new keto-intermediate was detected at higher reaction temperatures. Due to the newly detected intermediate (xylulose), the reaction network applied in previous work for xylose dehydration in HLW was expanded.[18] Additionally, a minor difference was observed in the distribution of isomerization products, with xylulose and ribulose identified as the corresponding keto-isomers of xylose and arabinose, respectively.[28] The final product distribution indicates a higher stability of arabinose, which appeared to be less readily converted towards furfural in comparison to xylose. The difference in the stability of arabinose and xylose has been attributed to the steric positioning of hydroxyl groups, distribution of individual isomer as well as its anomeric form.[60] Xylose and arabinose are known to exist in an open configuration, or cyclic from of pyranose and furanose, that can appear in either α or β anomeric forms. In aqueous solutions, arabinose is majorly found in α-pyranose form that appears to be more stable compared to more readily available β-pyranose form like in the case of xylose.[25] H1-NMR spectrum of individual pentoses, demonstrating the difference in the ratio of α and β anomeric form can be found in Supporting Information, Figure S26.

Subsequently, the calculated kinetic parameters confirmed the superior stability of arabinose in comparison to xylose. This is indicated by a lower reaction rate constant, k1, for the direct conversion to furfural, as shown in Table 2. Additionally, arabinose derived humin formation exhibited a slower reaction rate ($k_{3a}=2.4\times10^{-4}$) compared to xylose ($k_{3x}=4.7\times10^{-4}$) at 175 °C, while its slightly lower activation energy (121 kJ mol^{-1}) suggests slower arabinose degradation at higher temperatures. Comparable Ea were reported by Gairola et al. for the arabinose dehydration and its degradation with 112 kJ mol^{-1} and 121 kJ mol^{-1}, respectively.[61] Furthermore, the isomerization of xylose and arabinose proceeded at similar rates (k_{4x}/k_{4xr} vs k_{4a}/k_{4ar}), with a slightly higher activation energy for xylulose formation (162 kJ mol^{-1}). The conversion of arabinose and its intermediates exhibited lower activation energies compared to the conversion of xylose and xylulose.[25] Overall, both ketopentoses exhibited faster degradation compared to aldopentoses, a finding also reported by Ershova et al.[50]

The catalyst-free environment for pentose dehydration in HLW thus proved to be favorable for the formation of furfural by achieving significant yields. Therefore, the prevalence of pentose dehydration in HLW should not be neglected, especially at higher temperatures.

Sulfuric Acid Catalyzed Dehydration of Pentoses

Sulfuric acid is one of the most frequently employed mineral acids for acid-catalyzed saccharide dehydration reactions. It is typically utilized in the pre-treatment process of the lignocellulosic biomass fractionation and therefore, is commonly present in final hemicellulose streams.[8] To assess the effect of sulfuric acid dehydration reactions were conducted under two distinct reaction conditions. This approach prevented saccharide degradation in the absence of a catalyst at lower temperatures and allowed the determination of kinetic parameters, particularly for sulfuric acid-catalyzed dehydration. Initially, pentose dehydration was carried out in the lower temperature range of 120–

Table 2. Calculated kinetic parameters (reaction rate constant and activation energies) for xylose and arabinose conversion in three different reaction medium. * Refers to the values calculated from [18].

	Calculated reaction rate constants at 175 °C and activation energies in hot liquid water [min^{-1}, $kJ\,mol^{-1}$]		Calculated reaction rate constants at 175 °C and activation energies in sulfuric acid [$mol\,L^{-1}\,min^{-1}$, $kJ\,mol^{-1}$]		Calculated reaction rate constants at 130 °C and activation energies in formic acid [$mol\,L^{-1}\,min^{-1}$, $kJ\,mol^{-1}$]	
Starting feedstock	Xylose	Arabinose	Xylose	Arabinose	Xylose	Arabinose
k1	2.5×10^{-3}	1.5×10^{-3}	7.6×10^{-1}	4.3×10^{-1}	5.1×10^{-2}	2.4×10^{-2}
Ea_1	136	108	156	151	123	115
k2	9.8×10^{-4}*	9.8×10^{-4} *	7.8×10^{-2}	7.8×10^{-2}	5.6×10^{-3}	5.6×10^{-3}
Ea_2	71 *	71 *	91	91	107	107
k3	4.7×10^{-4}	2.4×10^{-4}	1.9×10^{-1}	1.2×10^{-2}	3.8×10^{-3}	1.1×10^{-2}
Ea_3	158	121	168	166	146	111
k4	2.4×10^{-3}	2.7×10^{-3}	3.0×10^{-1}	3.2×10^{-2}	/	/
Ea_4	162	121	164	115		
kr4	1.3×10^{-2}	1.5×10^{-2}	2.4×10^{-1}	1.1×10^{-2}	/	/
Ear_4	167	221	94	191		
k5	2.2×10^{-2}	2.3×10^{-2}	2.1	1.0	/	/
Ea_5	92	69	40	37		
k6	2.3×10^{-2}	2.7×10^{-2}	1.3×10^{-1}	5.5×10^{-1}	/	/
Ea_6	142	67	41	40		

140 °C using three different H_2SO_4 concentrations (5, 10, 50 g/L). Subsequently, higher temperatures (160–190 °C) were also used for the H_2SO_4-catalyzed pentose dehydration to validate the model in a broader temperature range where the previously calculated kinetic parameters obtained for pentose conversion in HLW was also considered. Time dependent concentration profiles of both arabinose and xylose during activity tests carried out at all the studied temperatures and acid concentrations are depicted in Figure S7 and S8 within the Supporting Information.

The dehydration of both aldo-pentoses (xylose and arabinose) exhibited the trend of strong temperature and acid concentration dependency. Notably, no isomerization products were detected under conditions of low temperature and high acid concentration, depicted in Supporting Information (Figure S7(d–i) and 8(d–i)). Nevertheless, both pentoses tended to undergo isomerization at higher temperatures (160–190 °C) and the addition of 1 g/L of H_2SO_4, which is demonstrated in Supporting Information (Figure S7(a–c) and 8(a–c)). The proposed reaction network was therefore considered to follow exactly as presented in Figure 1.

Within the lower temperature range of 120–140 °C, xylose dehydration resulted in the highest furfural yield of 50 mol% (140 °C, 2 hours and 50 g/L of H_2SO_4), as shown in Figure 2. A similar furfural yield was reported by Krzelj et al. under comparable reaction conditions.[13] As the temperature range was extended further to 160–190 °C and the H_2SO_4 concentration was reduced to 1 g/L, furfural yield increased further, reaching 59 mol% after 75 minutes at 190 °C. This is comparable to what has been reported elsewhere by Erchova et al.[50]

Nevertheless, arabinose again demonstrated superior stability over xylose, resulting in overall lower conversion and furfural yield when using H_2SO_4 as a catalyst, as determined previously (Figure 2).[60]

The difference in pentose stability is shown by the difference in the calculated kinetic parameters, where xylose dehydration to furfural ($k_{1x} = 7.6\times10^{-1}\,mol\,L^{-1}\,min^{-1}$) appeared to be faster compared to arabinose dehydration ($k_{1a} = 4.3\times10^{-1}\,mol\,L^{-1}\,min^{-1}$) towards furfural, with similar activation energies (Table 2). Furthermore, it was determined that both xylose-derived humin formation (k_3) and isomerization (k_4) tended to proceed considerably faster in comparison to arabinose. This aligns with several other findings where the reaction rate constant for arabinose conversion was approximately half that of xylose.[19,62,63] In terms of dehydration, the addition of H_2SO_4 resulted in a notable increase in reaction rates. More specifically, reaction rates for direct arabinose and xylose dehydration (k_{1x} and k_{1a}) and furfural-derived humin formation (k_2) exhibited the most significant increase. Correspondingly, Erchova et al. reported xylulose dehydration to furfural to proceed the fastest, followed by its degradation.[50] Furthermore, xylulose and ribulose dehydration to furfural as well as their degradation proceeded substantially faster with decreased activation energy (Ea). The calculated activation energies for xylose conversion were found to be similar by Krzelj et al.[13] Likewise, the activation energies for arabinose dehydration were estimated to be in the same range (109 to 133 $kJ\,mol^{-1}$) as reported by Danon et al., Gairola et al., and Zhao et al.[19,52,61]

Although high furfural yields were observed in a catalyst-free environment, the addition of low H_2SO_4 concentration improved and enabled a maximum furfural yield at higher reaction temperatures (190 °C). This indicates the possibility of efficient furfural formation from crude hemicellulose streams

directly from the Organosolv process without modification or addition of organic solvent.[64] On the other hand, operating at low temperatures would require high H_2SO_4 acid concentration to achieve comparable furfural yields, which is generally to be avoided.[13]

Formic Acid Catalyzed Dehydration of Pentoses

In addition to mineral acids such as sulfuric acid, weaker organic acids have also been utilized for the conversion of saccharides.[65,66] Particularly, formic acid has been frequently used commercially not only as an acid catalyst but also as a fractionation solvent during the Organosolv biomass pre-treatment in the Milox and Formosolv processes.[25,67] The hemicellulose fractions produced by these processes are commonly rich in formic acid. Therefore, the subsequent objective was to study the dehydration of hemicellulose-derived saccharides utilizing formic acid as a catalyst and reaction solvent.

The conversion of arabinose and xylose was studied in three distinct formic acid concentrations (25 wt./vol.%, 50 wt./vol.% and 75 wt./vol.%), within the temperature range of 120–140 °C. The results following activity tests are displayed in Figures S9–10 within the Supporting Information. Overall, analogous to the reactions conducted under hydrothermal conditions with and without H_2SO_4, a consistent pattern of increased furfural yield and pentose conversion was observed with rising temperature and acid concentration.

Both pentoses were dehydrated directly to furfural in a formic acid solution without detecting any isomerization products. As a result, the reversible isomerization reaction steps were omitted from the reaction network. Nevertheless, k_1, k_2, and k_3 continue to correspond to the reaction rate constants for the dehydration of xylose/arabinose to furfural and the formation of degradation products/humins from xylose/arabinose, and furfural, respectively. Remarkably, the furfural yield that was achieved at 140 °C with the highest formic acid concentration surpassed the maximum furfural yield achieved with sulfuric acid. Specifically, xylose dehydration resulted in 67 mol% after 5 hours, while arabinose yielded only 45 mol% furfural under identical operating conditions (Figure 3). Correspondingly, formic acid was found to enable higher furfural yield during xylose dehydration compared to H_2SO_4, as reported by Almhofer.[68]

Based on the kinetic parameters of formic acid catalyzed pentose conversion, arabinose appears less readily converted to furfural with slower reaction rates for furfural and humin formation. On the other hand, those same reaction steps when catalyzed by formic acid demonstrated lower Ea compared to H_2SO_4, suggesting a reduced temperature dependence. Both trends are consistent with observations made by Dussan et al., who highlighted the difference in pentose reactivity. They reported that arabinose was less reactive, in addition to the reduced temperature sensitivity of formic acid catalyzed sugar conversion.[25] In contrast, furfural degradation exhibited the lowest activation energy (107 kJ mol^{-1}) when carried out in the formic acid medium. The obtained kinetic parameters are consistent with findings by Lamminpää et al., with Ea ranging between 76 and 161 kJ mol^{-1} for formic acid-catalyzed xylose conversion whereas furfural degradation exhibiting the lowest Ea.[69]

Overall, both pentoses demonstrated the ability to be converted to furfural under the various tested reaction conditions. The main difference occurs between their reactivity due to the variation in the steric position of the −OH groups due to their different distribution of tautomeric forms. When comparing the reaction rate constants at the same temperature of 130 °C, it is notable that formic and sulfuric acid catalyzed

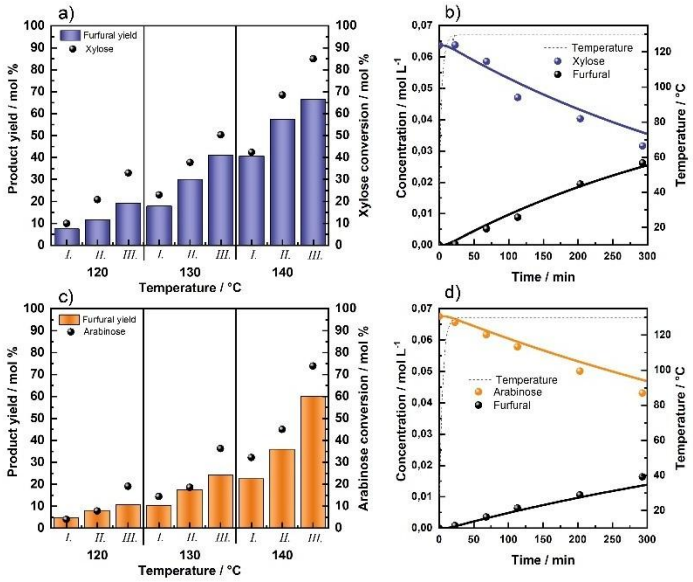

Figure 3. Maximal furfural yield and a) xylose and c) arabinose conversion at different temperatures where I., II., III., IV., correspond to acid concentrations of 25, 50 and 75 wt./vol.%. Product distribution as a function of the time for the b) xylose and d) arabinose dehydration reaction in mixture of formic acid and water (75 wt./vol.%) at 130 °C.

furfural degradation exhibit similar reaction rate constants (Supporting Information, Table S3). Importantly, dehydration of both pentoses appears to be significantly enhanced with the addition of formic acid, resulting in a significantly higher reaction rate constant for direct pentose dehydration to furfural.

The use of formic acid most likely influenced the reaction kinetics not only as a catalyst but also as a reaction solvent as it was present in considerable amounts.[70] Particularly in the case of xylose dehydration, formic acid increased the yield of furfural, even at a relatively low reaction temperature (140 °C). This would suggest that Milox or Formosolv derived hemicellulose have the potential to be efficiently converted to furfural without added acids.[2,25,68]

Mechanism of Hexose Dehydration

In addition to pentoses, hexoses such as glucose, galactose, and mannose are known to be present within the hemicellulose fraction, which offers an additional valorization route towards 5-hydroxymethylfurfural, levulinic acid as well as anhydrosugars such as levoglucosan.[31,71] Unlike ketohexoses, aldohexoses are known to be less reactive and more difficult to selectively convert into furanics.[18,72] Due to their aldehyde functionality, the C1 atom remains a part of the pyranose ring that, after an initial protonation, can consequentially result in the generation of a resonance-stabilized carbocation. Subsequently, this carbocation then may substantially enhance undesired side reactions leading to the formation of polymeric species.[12] To obtain relevant information regarding further process optimization, reaction kinetics hexoses (glucose, mannose and galactose) were investigated under hydrothermal reaction conditions, both in the absence and presence of sulfuric and formic acid.

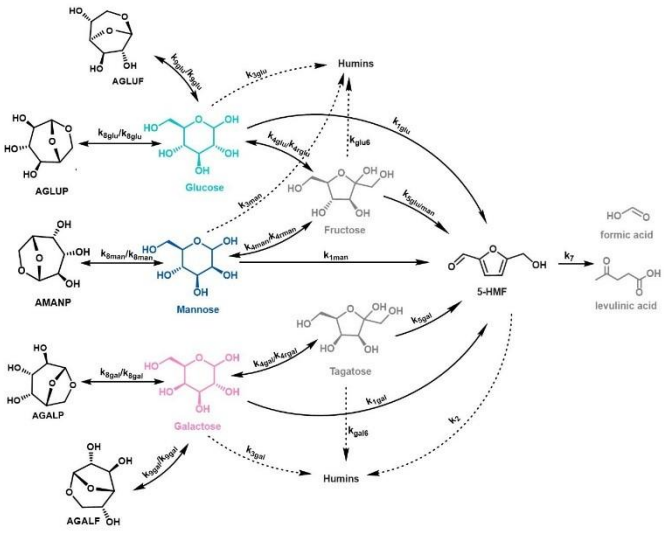

Figure 4. Proposed reaction network of hexose (glucose, mannose and galactose) conversion.

The proposed reaction mechanism is presented in Figure 4, which considers all the quantifiable liquid products.

All three aldohexoses were predominantly dehydrated to HMF, and their corresponding reaction rate constants are denoted as k_{1glu}, k_{1ga}l and k_{1man}. In addition to the dehydration step, all three saccharides tended to undergo isomerization to their respective keto-isomers. For example, mannose and glucose reversibly isomerize (k_{4glu}/k_{4rglu} and k_{4man}/k_{4rman}) to fructose, whereas galactose isomerizes to tagatose (k_{4gal}/k_{4rgal}).[28,73] Both keto-isomers can later undergo dehydration to HMF ($k_{5glu} = k_{5ma}$n and k_{5gal}).[72] Additionally, all of the hexoses and HMF ultimately decompose to undesirable by- products, commonly referred to as humins.[74] Specific reactions in the presented reaction scheme are described as k_{3glu}, k_{3man}, and k_{3gal} for humin formation derived from glucose, mannose, and galactose, respectively, whereas $k_{6glu} = k_{6man}$, k_{6gal} and k_2 correspond to the degradation of fructose, tagatose and HMF to humins. When an acidic environment was introduced by adding formic and sulfuric acid, HMF not only appeared to be degraded into humins but was rather converted into levulinic acid.[75,76] This rehydration reaction is described by the reaction rate constant k_7.

As sulfuric and formic acids were added as catalysts, anhydrosaccharides were detected as additional dehydration by-products. In the case of acid-catalysed glucose dehydration, 1,6-anhydro-β-glucopyranose or levoglucosan (AGP) and 1,6-anhydro-β-glucofuranose (AGF) were identified.[16,30] Similarly, 1,6-anhydro-β-galactopyranose (AGALP) and 1,6-anhydro-β-galactofuranose (AGALF) were detected as by-products during galactose conversion, while only 1,6-anhydro-mannopyranose (AMP) was observed during mannose dehydration.[42,77] Hence, the reactions leading to anhydrosaccharide formation were considered to be reversible.[16] Reversible conversion of glucose-AGP and glucose-AGF were denoted as k_{9glu}/k_{9rglu} and k_{8glu}/k_{8rglu}. The isomerization of galactose to AGALP and AGALF was described by k_{8gal}/k_{8rgal} and k_{9gal}/k_{9rgal}, respectively, while mannose-AMP conversion was demonstrated by k_{8man}/k_{8rman}, as depicted in Figure 4. The formation of anhydrosaccharides was more pronounced in formic acid, whereas it was relatively scarce when sulfuric acid was used. Therefore, the formation of anhydrofuranose saccharides was omitted from the model for sulfuric acid catalyzed hexose dehydration due to their negligible concentrations.

Similarly to pentose dehydration, no keto-isomers (fructose and tagatose) were detected during formic acid hexose dehydration at 120–140 °C and therefore, were not considered in the reaction network for this reaction media.[25] This could be attributed to the rapid isomerization that made keto-isomers undetectable, or that isomerization does not tend to proceed at lower temperatures.

Dehydration of Hexoses in Hot Liquid Water

Despite superior stability of aldohexoses in comparison to aldopentoses, significant hexose conversion has been reported during hydrothermal hexose degradation in HLW with the

formation of different dehydration and isomerization products.[28,56,78] Both glucose and fructose demonstrated a strong temperature-dependent conversion when temperatures are increased above 145 °C in a catalyst-free environment.[18]

To investigate the kinetics of two additional hexoses (mannose and galactose) conversion in aqueous media, dehydration experiments were conducted without a catalyst within the temperature range of 160–190 °C (Supporting Information, Figure S13–14). Likewise, dehydration of both mannose and galactose displayed a strong temperature dependency, with both saccharide conversion and HMF yield increasing with raising reaction temperature. Under these specific catalyst-free reaction conditions, HMF was the dominant final product as it was unable to rehydrate further into levulinic acid due to the absence of an acidic catalyst.[76,79]

Furthermore, a maximum conversion of mannose and galactose reached 82 mol% and 75 mol% after a reaction time of 5 hours at 190 °C, whereas the highest HMF yields (36 mol% and 29 mol%) were achieved at a shorter reaction time (2–3 h) for mannose and galactose, respectively (Figure 5). Both the conversion and HMF yields were comparable to those reported previously for the dehydration of glucose under hydrothermal reaction conditions.[18] Under the tested hydrothermal reaction conditions, all three aldohexoses demonstrate the ability to isomerize into their respective keto-isomers. Similarly, Usuki et al. reported isomerization of glucose, fructose and mannose in so-called subcritical water in the temperature range of 180–240 °C.[78] Notably, the isomerization of mannose-fructose in this study appeared to be more pronounced than the isomerization of glucose-fructose reported previously.[18] Correspondingly, Lü et al. reported similar isomerization of hexose (galactose, glucose and mannose) in a continuous reactor set up in hot compressed water in the temperature range of 160–250 °C.[28] The authors reported an analogous trend in the amount of respective isomer formed, with mannose resulting in the highest concentration of fructose. Similar to mannose, galactose also demonstrated an additional step of isomerization towards tagatose, which can be later dehydrated to HMF due to its ketohexose form .[12,42,80] Isomerization of galactose into its respective keto-hexose, tagatose, is often more pronounced in the presence of a basic or Lewis acid catalyst.[73,81] Despite this, it was also observed under these particular hydrothermal reaction conditions.

Interestingly, galactose dehydration resulted in slightly lower conversion and a maximum yield of HMF compared to glucose or mannose.[12,18,82] The variation in HMF yield and galactose conversion may be attributed to differences in the rate and selectivity of tagatose dehydration to HMF, as suggested by Van Putten et al.[72]

Calculated kinetic parameters for mannose dehydration in hot liquid water followed a similar trend to those reported for glucose dehydration.[18] Likewise, fructose dehydration ($k_{5man} = 1.2\times10^{-2}\ min^{-1}$) to HMF proceeded the fastest. Mannose isomerization to fructose ($k_{4man} = 4.5\times10^{-3}\ min^{-1}$) progressed more rapidly, with higher Ea (163 kJ mol^{-1}), compared to its direct conversion to HMF ($k_{1man} = 1.8\times10^{-3}\ min^{-1}$). Reaction rate constant for mannose-derived humin formation appeared to be the slowest, with the lowest activation energy (48 kJ mol^{-1}). This is consistent with the values reported by Swift et al. for acid catalysed glucose dehydratoin.[83]

Alternatively, galactose dehydration to HMF ($k_{1gal} = 1.0\times10^{-3}\ min^{-1}$) seemed to be the slowest out of all three hexoses, while the dehydration of tagatose to HMF ($k_{5gal} = 2.5\times10^{-2}\ min^{-1}$) appeared to be the fastest under these conditions. However, the inferior HMF yield could be also attributed to the fastest reaction rate constant of tagatose degradation to humins (k_{5gal}). However, comparing the degradation of hexoses to humin galactose degradation was found to occur the slowest (k_{3gal}) with the highest activation energy (101 kJ mol^{-1}).

Overall, hydrothermal conditions allowed hexose isomerization even without added catalyst and a significant, albeit non-selective, conversion of hexoses to HMF was also exhibited.

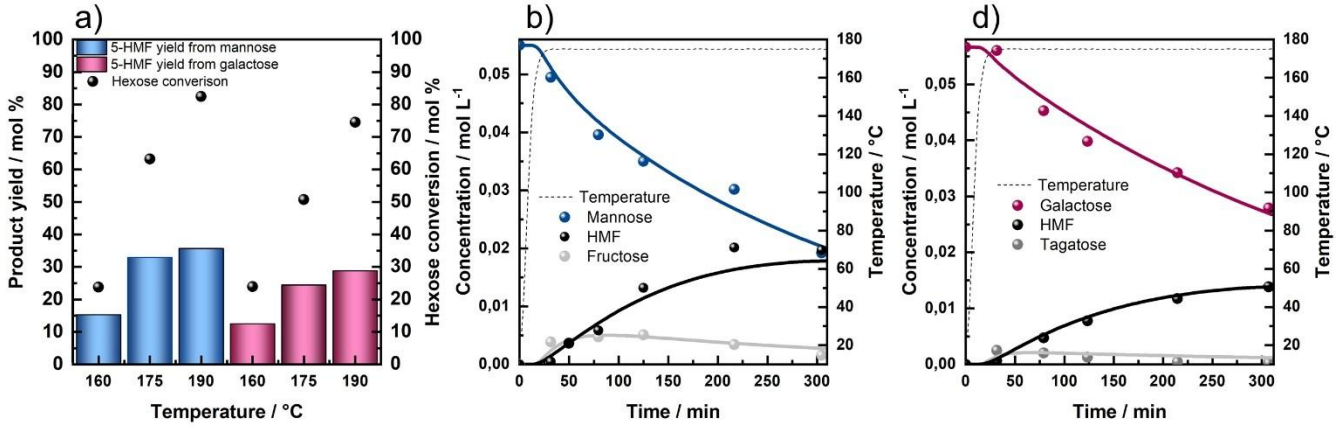

Figure 5. a) Maximal HMF yield, mannose and galactose conversion at different temperatures in HLW and product distribution as a function of the time for the b) mannose and d) galactose in HLW at 175 °C.

Sulfuric Acid Catalyzed Dehydration of Hexoses

Similar to pentoses, glucose, mannose and galactose were also dehydrated under acidic conditions at two different temperature ranges (120–140 °C and 160–190 °C), depicted in Figure S15–17 within the Supporting Information. Depending on the reaction conditions chosen, the distribution of the liquid products differed considerably. In the lower temperature range and high sulfuric acid concentrations (5–50 g/L), HMF yield was almost negligible, while levulinic acid appears as the thermodynamically favoured product of all three hexoses. Due to the high acid concentration, it can be assumed that the isomerization reaction proceeded rapidly and the intermediates such as fructose and tagatose could not be detected, similar to what has been reported elsewhere.[16,42] However, the formation of both ketohexoses was observed when carried out at the higher reaction temperature range and lower acid concentration (1 g/L).

Glucose conversion demonstrated strong acid and temperature dependence. When the acid concentration and temperature were increased to 50 g/L and 140 °C, the dehydration of glucose resulted in 46 mol% of levulinic acid and 70 mol% of glucose conversion. In the higher temperature range of 160–190 °C with a lower acid concentration, the yield of levulinic acid slightly decreased to 41 mol%, while glucose conversion approached nearly 100 mol% after 5 hours at 190 °C.

Conversely, higher temperatures and lower acid concentration led to a substantially increased HMF yield (19 mol%) achieved within 75 minutes at 190 °C (Figure 6). Based on the calculated kinetic parameters, it can be observed that the rehydration of HMF ($k_7 = 1.2\ L\,mol^{-1}\,min^{-1}$) and fructose dehydration towards HMF ($k_{5glu} = 2.5\ L\,mol^{-1}\,min^{-1}$) proceeds the fastest. Additionally, the reverse reactions involving levoglucosan were also detected during sulfuric acid catalyzed glucose dehydration.[16] Likewise, the reversion reactions (k_{8glu}/k_{8rglu}) proceeded rapidly with high reaction rate constants, especially in the case of levoglucosan with the lowest calculated activation energies (66 and 35 kJ mol^{-1}, for Ea_8 and Ea_{8r}, respectively). Furthermore, Toif et al. reported similar reaction rate constants for glucose conversion to levugucosan,[84] while Abdilla et al. demonstrated comparable reaction rates for levoglucosan to glucose conversion.[32] Additionally, the formation of humins from glucose appeared to be significantly more pronounced with noticeably lower activation energy in acidic media as opposed to catalyst-free glucose dehydration.

Mannose yielded a maximum of 45 mol% levulinic acid under two different reaction conditions, firstly at 140 °C, 50 g/L H_2SO_4, 5 h and secondly at 190 °C, 1 g/L H2SO4, 5 h (Figure 6). Similar to glucose, mannose also resulted in a significant amount of HMF (24 mol%, 175 °C, 75 min), at elevated temperature and lower acid concentration. In contrast to the dehydration of glucose, mannose dehydration has not been frequently described in the literature. As mentioned earlier, glucose and mannose share fructose as their ketohexose isomer and thus, are often assumed to have similar reactivity.[83,85] Even though no isomerization/epimerization products (glucose/fructose) were detected in dehydration reactions with mannose

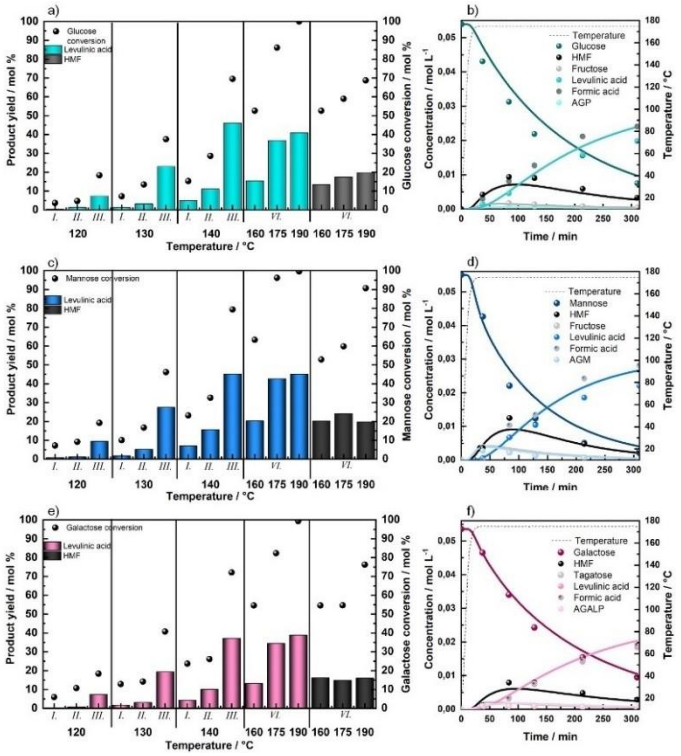

Figure 6. Maximal HMF and levulinic acid yield and a) glucose, c) mannose and e) galactose conversion at different temperatures where I., II., III., IV., correspond to acid concentrations of 5, 10, 50 and 1 g/L, b), d), f) product distribution as a function of the time for the glucose, mannose and galactose conversion catalyzed by H_2SO_4 (1 g/L) at 175 °C.

below 160 °C, an increase in reaction temperature and decrease in acid concentration resulted in substantial mannose isomerization.[83,85] Additionally, reactions of mannose isomerization to fructose (k_{4man}) and anhydrosaccharide (k_{8man}) formation occurred faster than the analogous reversible reactions involving glucose. However, the concentration of anhydromannose under these specific conditions and did not exceed 5 mol% due to high value of reversible rate constant (k_{8rman}). The calculated kinetic parameters for mannose dehydration appear to be similar to the parameters determined for glucose conversion, confirming the assumption of similar hexose reactivity. However, mannose resulted in a higher conversion in comparison to glucose, especially within the temperature range of 160–190 °C, (Figure 6). This aligns with the notable higher reaction rate constant for mannose degradation towards humins ($k_{3man} = 3.2{\times}10^{-2}\ L\,mol^{-1}\,min^{-1}$), compared to glucose derived humin formation ($k_{3glu} = 6.0{\times}10^{-3}$ L mol^{-1} min^{-1}), as shown in Table 3.

According to HPLC analysis, galactose dehydration proceeded similarly to mannose and glucose, with tagatose and HMF as intermediates, anhydrogalacto-furanose and pyranose as reversible by-products, and levulinic acid as an end product. The highest yield of levulinic acid (~38 mol%) using galactose as the starting substrate was achieved under

both low temperature and high H_2SO_4 concentration (140 °C and 50 g/L H_2SO_4) as well as under high temperature and low

Table 3. Calculated kinetic parameters (reaction rate constant and activation energies) for glucose, mannose and galactose conversion in three different reaction medium. * Refers to the values calculated from [18].

	Calculated reaction rate constants at 175 °C and activation energies in hot liquid water [min^{-1}, kJ mol^{-1}]			Calculated reaction rate constants at 175 °C and activation energies in sulfuric acid [L mol^{-1} min^{-1}, kJ mol^{-1}]			Calculated reaction rate constants at 130 °C and activation energies in formic acid [L mol^{-1} min^{-1}, kJ mol^{-1}]		
	Glucose*	Mannose	Galactose	Glucose	Mannose	Galactose	Glucose	Mannose	Galactose
k1	1.4×10^{-3}	1.8×10^{-3}	1.0×10^{-3}	1.9×10^{-1}	1.4×10^{-1}	1.4×10^{-1}	1.3×10^{-2}	1.8×10^{-2}	1.6×10^{-2}
Ea_1	85	117	125	158	148	173	139	143	145
k2	3.6×10^{-3}	3.6×10^{-3} *	3.6×10^{-3} *	5.4×10^{-1}	5.4×10^{-1}	5.4×10^{-1}	6.5×10^{-2}	6.5×10^{-2}	6.5×10^{-2}
Ea_2	106	106	106	107	107	107	91	91	91
k3	2.9×10^{-7}	6.0×10^{-7}	5.6×10^{-8}	6.0×10^{-3}	3.2×10^{-2}	1.7×10^{-2}	4.5×10^{-3}	1.3×10^{-3}	2.1×10^{-3}
Ea_3	78	48	101	62	107	61	106	119	102
k4	1.2×10^{-3}	4.5×10^{-3}	3.0×10^{-3}	4.6×10^{-2}	2.7×10^{-1}	1.0×10^{-1}	/	/	/
Ea_4	98	163	147	174	169	167			
k4r	1.4×10^{-3}	2.3×10^{-3}	3.5×10^{-2}	5.1×10^{-1}	1.7×10^{-3}	2.7×10^{-2}	/	/	/
Ea_{4r}	120	153	140	93	27	47			
k5	1.2×10^{-2}	1.2×10^{-2}	2.5×10^{-2}	2.5	2.5	1.3	/	/	/
Ea_5	139	139	103	31	31	78			
k6	1.3×10^{-3}	1.3×10^{-3} *	1.0×10^{-2}	3.8×10^{-2}	3.8×10^{-2}	1.7×10^{-2}	/	/	/
Ea_6	108	108 *	55	32	32	70			
k7	/	/	/	1.2	1.2	1.2	7.6×10^{-2}	7.6×10^{-2}	7.6×10^{-2}
Ea_7				86	86	86	91	91	91
k8	/	/	/	3.6×10^{-2}	6.3×10^{-1}	9.3×10^{-2}	1.6×10^{-1}	7.2×10^{-1}	1.7×10^{-1}
Ea_8				66	76	83	40	78	87
k8r	/	/	/	2.2	6.2	1.8	3.9	11.5	4.2
Ea_{8r}				35	43	83	36	46	70
k9	/	/	/	/	/	/	2.2×10^{-1}	/	3.1×10^{-1}
Ea_9							35		50
k9r	/	/	/	/	/	/	6.2	/	3.3
Ea_{9r}							36		41

H_2SO_4 concentration (190 °C and 1 g/L H_2SO_4). However, this levulinic acid yield was notably lower in comparison to what was achieved using glucose and mannose (Figure 6). The levulinic acid yield that was obtained in this study aligns well with a study published by Martina et al. who investigated the kinetics of galactose conversion using sulfuric acid, achieving a maximum levulinic acid yield at 140 °C.[42] Additionally, Ringgani et al. reported the highest galactose yield when using sulfuric acid at 170 °C after only 40-minutes.[80]

However, the yield of HMF appeared to not exceed 16 mol% and was achieved after 75 min and 190 °C. Studies by Kim et al. and Hu et al. suggest that the different steric configuration of −OH groups in galactose intermediates (tagatose) formed by isomerization could explain the lower HMF and levulinic acid yields compared to mannose and galactose.[82,86] Although the galactose isomerization towards tagatose proceeds rapidly, its further dehydration to HMF occurs slower compared to fructose dehydration, thus leading to a lower final HMF yield during galactose conversion.

The assumptions regarding less favorable galactose dehydration towards HMF and levulinic acid can be confirmed by the following calculated kinetic parameters. The reaction rate constant for anhydrogalactose formation ($k_{8gal} = 9.3\times10^{-2}$ L mol^{-1} min^{-1}) appears to be notably higher compared to anhydroglucose ($k_{8glu} = 3.6\times10^{-2}$ L mol^{-1} min^{-1}) formation but still lower than the formation of anhydromannose ($k_{8man} = 6.3\times10^{-1}$ L mol^{-1} min^{-1}). Additionally, it exhibits a significantly lower reversible reaction rate constant (k_{8rgal}) in comparison to the reverse reactions of anhydroglucose and mannose. Correspondingly, acid-catalyzed galactose conversion led to higher amounts of anhydrogalactose products.

The addition of sulfuric acid overall negatively impacted HMF yield, facilitating its rehydration and enhancing the formation of levulinic acid. Therefore, depending on acid concentration, levulinic acid was demonstrated to be the most viable targeted product derived from C6 using an Organosolv fractionation feedstock. However, an acid-free aqueous environment could be more suitable for the production of HMF.

Formic Acid Catalyzed Dehydration of Hexoses

Organic acids are not only commonly utilized as lignocellulose fractionation solvents, but are also frequently utilized for hexose

dehydration to HMF.[11] De Souza reported the use of concentrated aqueous solutions of organic acids to convert fructose with high HMF yields (64 mol%).[66] Thus, formic acid-catalyzed dehydration reactions were carried out for all three selected hexoses: glucose, mannose, and galactose, in the temperature range of 120–140 °C and three different formic acid concentrations, and their results are shown in Figure S18–20 within the Supporting Information. When dehydration reactions were carried out in highly concentrated formic acid, the formation of anhydro-mannose, -glucose, and -galactose was especially pronounced. This would suggest an inhibitory role of water in anhydro-saccharide formation as has been described elsewhere.[87] The calculated kinetic parameters support this observation as reversible anhydrosaccharide formation reactions (k_{8glu} *and* $k_{9/k9r}$) proceeded with the highest reaction rate constants and the lowest activation energies (36–87 kJ mol^{-1}) for all studied hexoses when formic acid is present. Furthermore, galactose appeared to form a notable amount of anhydrosaccharides with up to 15 mol%.

Under these particular reaction conditions, aldohexose conversion followed the trend of glucose < galactose < mannose, with mannose achieving almost 60 mol%. Correspondingly, the direct dehydration of mannose appeared to proceed slightly faster, followed by galactose and glucose. Among hexoses, mannose dehydration resulted in the highest HMF yield (8 mol%) of all three of the studied hexoses, while the maximum yield of levulinic acid appeared to be comparable for all of the investigated hexoses, yielding around 15 mol% (Figure 7). Moreover, HMF rehydration (k_7) catalyzed by formic acid exhibited a reaction rate constant slightly lower but comparable to that of sulfuric acid-catalyzed conversion. Nonetheless, the rate constant ($k_7 = 7.6\times10^{-2}$ L mol^{-1} min^{-1}) of rehydration remained higher than the one of direct hexose dehydration ($k_{1glu/man/gal} = 1.3–1.8\times10^{-2}$ L mol^{-1} min^{-1}).

These results demonstrate that hexose conversion following formic acid Organosolv treatment would result in significant yields of three primary products; HMF, levulinic acid, and anhydrosugars. All three are known to be valuable platform chemicals with various potential applications, although it would still be essential to further optimize the yields of the individual compound to maximize their valorization.[88]

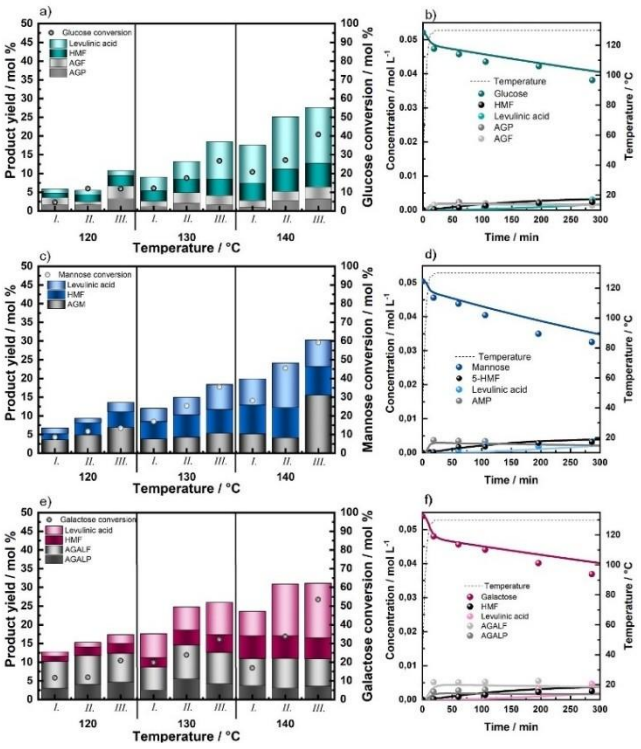

Figure 7. Maximal product yields and a) glucose, c) mannose and e) galactose conversion at different temperatures, where I., II., III., IV., correspond to acid concentrations of 25, 50 and 75 wt./vol.%, b), d) and f) product distribution as a function of the time for the glucose, mannose and galactose dehydration reaction in mixture of formic acid and water (75 wt./vol.%) at 130 °C.

Optimization of Organosolv Hemicellulose Dehydration

In order to validate the calculated kinetic parameters, intermediates (fructose, levoglucosan, levomannosan, levogalactosan) were used to estimate the correlation between experimental and predicted values, as demonstrated in the Supporting Information (Figures S21–23). Furthermore, mixtures of xylose and glucose in varying proportions were utilized for dehydration in various reaction media (HLW, formic and sulfuric acid), resulting in no significant effect on the kinetics of individual sugars, depicted in Supporting Information (Figure S24 and S25).

The established kinetic model and calculated kinetic parameters served as a tool for optimizing the process conditions of real hemicellulose streams obtained through two different methods of Organosolv fractionation, *H.S.* and *H.F.* Based on the saccharide (xylose, arabinose, glucose, galactose, mannose) and acid (sulfuric/formic) content present in the starting stream, optimal process conditions (time and temperature) were predicted using calculated kinetic parameters to achieve the maximum yield of desired products. Due to high industrial relevance and challenging production, HMF and furfural were determined as the targeted compounds. After the analysis of the hemicellulose fractions catalyzed by sulfuric acid (*H.S.*) and formic acid (*H.F.*), the initial concentration of glucose, mannose and galactose, as well as arabinose and xylose were inputted into the model, considering the acid concentration of the stream as the starting parameters, to identify the optimal reaction conditions to achieve the maximum HMF and furfural yield.

In the case of *H.S.* process optimization, the model predicted the highest yield of both HMF and furfural to be achieved at the 233 °C at a reaction time of 28 min. This phenomenon can be explained by the relatively high activation energy and reaction rate constant for dehydration reaction, making the HMF and furfural formation more pronounced at elevated temperatures in comparison to other side reactions. As expected, the predicted HMF yield (33 mol%) appeared to be much lower compared to the maximum predicted furfural yield (69 mol%). The difference between the yields of furanics can be

attributed to the enhanced side reactions of degradation and HMF rehydration. A validation test was carried out to confirm the modelled predictions, where the hemicellulose stream (*H.S.*) was subjected to hydrothermal treatment at 245 °C for 35 min including the ramp-up time. The results obtained from the validation test agree very well with the predicted values.

Furthermore, the optimization of reaction parameters was performed for the second hemicellulose stream (*H.F.*) derived from formic acid-based fractionation. Given the difference in the reaction media, the kinetic parameters reported for formic acid catalyzed saccharide dehydration were used to predict the optimal conditions for achieving the maximum production of furfural. In this particular hemicellulose stream, HMF and levulinic acid were not considered as anticipated products for optimization due to the low hexose concentration. The optimized process conditions based on the composition of hemicellulose stream (H.F) substantially differed from those predicted for H.S. The optimal reaction time for H.F. appeared to be longer (75 min), while the reaction temperature tends to be significantly lower (175 °C), compared to reaction time and temperature predicted for H.S.

Subsequently, a validation test for formic acid-catalyzed saccharide dehydration was performed, confirming that a maximum furfural yield of can be achieved within 85 minutes at 175 °C. In this case, the experimental furfural concentrations tend to be slightly higher compared to the predicted values, Figure 8. This difference may be attributed to the presence of short-chain xylose/arabinose polysaccharides. Additionally, compounds such as salts and acid-soluble lignin could also affect the kinetics of saccharide conversion, although their contribution can be considered minor due to the highly diluted hemicellulose stream provided.[89] The optimization results are comparable with the predictions made by dos Santos Rocha, for the hydrotreatment of sugarcane and our previous study, which predicted short residence time and high temperature to achieve the highest yield of furanics.[24,18]

Conclusions

In this work, we have investigated the conversion of hemicellulose-derived pentoses (xylose and arabinose) and hexoses (glucose, mannose and galactose) to gain insight into the behavior of monosaccharide conversion under a wide range of conditions relevant to the utilization of hemicellulose directly after the Organosolv fractionation process. Therefore, three parallel kinetic models have been developed for hemicellulose derived monosaccharide conversion: i) in hot liquid water without added catalyst, ii) sulfuric acid and iii) formic acid-catalyzed reactions. The modelled values exhibited excellent agreement with the experimental results, providing data for further process optimization.

Both pentoses, xylose and arabinose, exhibited high furfural yields (45–59 mol%). Particularly elevated temperatures even in catalyst free aqueous environment lead to a substantial formation of furfural. The addition of sulfuric acid significantly influenced the distribution of the final products, primarily due to the overall increase in reaction rate constants, especially for pentose dehydration reactions. On the other hand, the addition of formic acid not only increased the reaction rate constant for pentose dehydration but also reduced its activation energy, which consequently led to high furfural yields achieved at significantly lower temperatures.

Hence, indicating that all three reaction conditions are suitable for further optimization of furfural formation.

The dehydration of hexoses generally exhibited a similar trend to that of pentoses, particularly in the reactions conducted in hot liquid water, which resulted in the highest HMF yield achieved under the tested reaction conditions. Contrarily, the addition of sulfuric acid resulted in the enhanced formation of levulinic acid. However, when formic acid was introduced to the reaction mixture, an increased formation of anhydrosaccharides was observed.

Results demonstrated that elevated temperatures (> 160 °C) and lower acid concentration can result in more substantial isomerization, while reactions conducted at lower temperatures seemed to proceed without an additional isomerization step, for all of the studied monosaccharides.

The introduction of an acidic environment also generally enhanced furfural and levulinic acid yields while reducing the required reaction time. The presence of acids also leads to a notable increase in saccharide conversion. However, it has a substantial effect on reducing the maximum HMF yield, primarily due to the rapid occurrence of rehydration reactions, which has proven to facilitate the production of levulinic acid.

Therefore, it can be concluded that the product distribution during hexose conversion was profoundly influenced by the reaction media and catalyst applied with various possibilities for the selection of targeted products (HMF, levulinic acid, anhydrosugars).

To validate the accuracy of the kinetic model, an optimization of process conditions was performed with two different real hemicellulose streams. The predicted values demonstrated an excellent correlation to experimental results. The sulfuric acid containing hemicellulose stream yielded 67 mol% of furfural and 33 mol% of HMF at 238 °C after 30 min, due to the relatively high Ea and reaction rate constant for direct sugar dehydration. In contrast, the conversion of hemicellulose stream that contained formic acid required a longer reaction time and

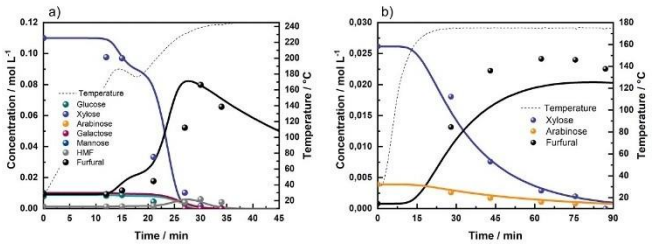

Figure 8. Validation experiments of (a) hydrothermal treatment of H.S derived by Ethanol-Ogranosolv treatment containing H_2SO_4 and (b) hydrothermal treatment of H.F. derived by Ogranosolv treatment using formic acid under the predicted optimal reaction conditions.

lower temperature (175 °C) to attain the maximum furfural yield (83 mol%).

Supporting Information

Concentration profiles of sugars under all of the tested conditions, can be found in supporting information.

Acknowledgments

The authors would like to appreciatively acknowledge the financial support of by the EU Framework Program for Research and Innovation Horizon 2020 under Grant agreement no. 887226 (BioSPRINT) and the Slovenian Research Agency (Program P2-0152 and the project J2-2492). Additionally, we would like to acknowledge the funding provided by the Slovenian Research Agency and German Academic Exchange Service (DAAD) for bilateral exchange project BI-DE/23-24-004 and would like to thank Fraunhofer-Zentrum für Chemisch-Biotechnologische Prozesse CBP for providing the hemicellulose stream, especially Ireen Gebauer.

Conflict of Interests

The authors declare no conflict of interest.

Data Availability Statement

The data that support the findings of this study are available from the corresponding author upon reasonable request.

Keywords: Kinetic modelling · Saccharide dehydration · Hemicellulose conversion · Levulinic acid · Hydroxymethyl(furfural)

[1] T. W. Walker, A. H. Motagamwala, J. A. Dumesic, G. W. Huber, *J. Catal.* **2019**, *369*, 518–525.
[2] K. J. Yong, T. Y. Wu, C. B. T. L. Lee, Z. J. Lee, Q. Liu, J. M. Jahim, Q. Zhou, L. Zhang, *Biomass Bioenergy* **2022**, *161*, 106458, DOI 10.1016/j.biombioe.2022.106458.
[3] K. I. Galkin, V. P. Ananikov, *ChemSusChem* **2019**, *12*, 2976–2982.
[4] M. Lang, H. Li, *ChemSusChem* **2022**, *15*, e202101531.
[5] L. T. Mika, E. Cséfalvay, Á. Németh, *Chem. Rev.* **2018**, *118*, 505–613.
[6] F. Carvalheiro, L. C. Duarte, F. M. Gírio, *J. Sci. Ind. Res.* **2008**, *67*, 849–864.
[7] S. C. Rabelo, P. Y. S. Nakasu, E. Scopel, M. F. Araújo, L. H. Cardoso, A. C. da Costa, *Bioresour. Technol.* **2023**, *369*, 128331, DOI 10.1016/j.biortech.2022.128331.
[8] P. Mäki-Arvela, T. Salmi, B. Holmbom, S. Willför, D. Y. Murzin, *Chem. Rev.* **2011**, *111*, 5638–5666.
[9] B. Danon, G. Marcotullio, W. De Jong, *Green Chem.* **2014**, *16*, 39–54.
[10] A. Morone, M. Apte, R. A. Pandey, *Renewable Sustainable Energy Rev.* **2015**, *51*, 548–565.
[11] L. Hu, Z. Wu, Y. Jiang, X. Wang, A. He, J. Song, J. Xu, S. Zhou, Y. Zhao, J. Xu, *Renewable Sustainable Energy Rev.* **2020**, *134*, 110317.
[12] T. Istasse, A. Richel, *RSC Advances* **2020**, *10*(40), 23720–23742.
[13] V. Krzelj, J. Ferreira Liberal, M. Papaioannou, J. Van Der Schaaf, M. F. Neira D'Angelo, *Ind. Eng. Chem. Res.* **2020**, *59*, 11991–12003.
[14] L. Kupiainen, J. Ahola, J. Tanskanen, *Ind. Eng. Chem. Res.* **2010**, *49*, 8444–8449.
[15] L. Kupiainen, J. Ahola, J. Tanskanen, *Chem. Eng. Res. Des.* **2011**, *89*, 2706–2713.
[16] B. Girisuta, L. P. B. M. Janssen, H. J. Heeres, *Chem. Eng. Res. Des.* **2006**, *84*, 339–349.
[17] W. Guo, Z. Zhang, J. Hacking, H. J. Heeres, J. Yue, *Chem. Eng. J.* **2021**, *409*, 128182.
[18] A. Jakob, B. Likozar, M. Grilc, *Green Chem.* **2022**, *24*, 8523–8537.
[19] B. Danon, W. Hongsiri, L. van der Aa, W. de Jong, *Biomass Bioenergy* **2014**, *66*, 364–370.
[20] A. H. Motagamwala, J. A. Dumesic, *Chem. Rev.* **2021**, *121*, 1049–1076.
[21] R. Šivec, M. Grilc, M. Huš, B. Likozar, *Ind. Eng. Chem. Res.* **2019**, *58*, 16018–16032.
[22] E. R. Garrett, B. H. Dvorchik, *J. Pharmaceutical Sci.* **1969**, *58(7),* 813–820.
[23] S. Rivas, M. J. González-Muñoz, V. Santos, J. C. Parajó, *Bioresour. Technol.* **2014**, *162*, 192–199.
[24] M. S. R. dos Santos Rocha, B. Pratto, R. de Sousa, R. M. R. G. Almeida, A. J. G. da Cruz, *Bioresour. Technol.* **2017**, *228*, 176–185.
[25] K. Dussan, B. Girisuta, M. Lopes, J. J. Leahy, M. H. B. Hayes, *ChemSusChem* **2015**, *8*, 1411–1428.
[26] D. Soukup-Carne, X. Fan, J. Esteban, *Chem. Eng. J.* **2022**, *442*, 136313, DOI 10.1016/j.cej.2022.136313.
[27] B. Cinlar, T. Wang, B. H. Shanks, *Appl Catal A Gen* **2013**, *450*, 237–242.
[28] X. Lü, S. Saka, *J. Supercrit. Fluids* **2012**, *61*, 146–156.
[29] J. E. Romo, K. C. Miller, T. L. Sundsted, A. L. Job, K. A. Hoo, S. G. Wettstein, *ChemCatChem* **2019**, *11*, 4715–4719.
[30] M. Ohara, A. Takagaki, S. Nishimura, K. Ebitani, *Appl Catal A Gen* **2010**, *383*, 149–155.
[31] I. Itabaiana Junior, M. Avelar Do Nascimento, R. O. M. A. De Souza, A. Dufour, R. Wojcieszak, *Green Chem.* **2020**, *22*, 5859–5880.
[32] R. M. Abdilla, C. B. Rasrendra, H. J. Heeres, *Ind. Eng. Chem. Res.* **2018**, *57*, 3204–3214.
[33] S. C. Rabelo, P. Y. S. Nakasu, E. Scopel, M. F. Araújo, L. H. Cardoso, A. C. da Costa, *Bioresour. Technol.* **2023**, *369*, 128331, DOI 10.1016/j.biortech.2022.128331.
[34] G. Tofani, E. Jasiukaitytė Grojzdek, M. Grilc, B. Likozar, *Green Chem.* **2023**, *26*, 186–201, DOI 10.1039/D3GC03274D.
[35] J. Köchermann, J. Mühlenberg, M. Klemm, *Ind. Eng. Chem. Res.* **2018**, *57*, 14417–14427.
[36] V. Choudhary, A. B. Pinar, S. I. Sandler, D. G. Vlachos, R. F. Lobo, *ACS Catal.* **2011**, *1*, 1724–1728.
[37] X. Chang, J. Zhang, R. Wu, X. Zhao, *Molecules* **2021**, *26*(9), 2753, DOI 10.3390/molecules26092753.
[38] S. Dapã, V. Santos, J. C. Parajã, *Study of Formic Acid as an Agent for Biomass Fractionation* **2002**, *22*(3), 213–221.
[39] H. Qiao, Y. Wang, Z. Ma, M. Han, Z. Zheng, J. Ouyang, *Bioresour. Technol.* **2023**, *374*, 128747, DOI 10.1016/j.biortech.2023.128747.
[40] A. Sluiter, B. Hames, R. Ruiz, C. Scarlata, J. Sluiter, D. Templeton, D. Crocker, *Determination of Structural Carbohydrates and Lignin in Biomass: Laboratory Analytical Procedure (LAP); Issue Date: April 2008; Revision Date: July 2011 (Version 07–08-2011)*, **2011**.
[41] A. Sluiter, B. Hames, R. Ruiz, C. Scarlata, J. Sluiter, D. Templeton, *Determination of Sugars, Byproducts, and Degradation Products in Liquid Fraction Process Samples: Laboratory Analytical Procedure (LAP); Issue Date: 12/08/2006*, **2006**.
[42] A. Martina, H. H. Van De Bovenkamp, I. W. Noordergraaf, J. G. M. Winkelman, F. Picchioni, H. J. Heeres, *Ind. Eng. Chem. Res.* **2022**, *61*, 9178–9191.
[43] K. Dussan, B. Girisuta, M. Lopes, J. J. Leahy, M. H. B. Hayes, *ChemSusChem* **2015**, *8*, 1411–1428.
[44] L. Kupiainen, J. Ahola, J. Tanskanen, *Ind. Eng. Chem. Res.* **2012**, *51*, 3295–3300.
[45] M. H. Kim, C. S. Kim, H. W. Lee, K. Kim, *Journal of the Chemical Society - Faraday Transactions* **1996**, *92*, 4951–4956.
[46] A. G. Dickson, D. J. Wesolowski, D. A. Palmer, R. E. Mesmer, *Dissociation Constant of Bisulfate Ion in Aqueous Sodium Chloride Solutions to 250°C*, **1990**.
[47] M. J. Antal, T. Leesomboon, W. S. Mok, G. N. Richards, *Carbohydr. Res.* **1991**, *217*, 71–85.
[48] X. Fang, M. P. Andersson, Z. Wang, W. Song, S. Li, *Carbohydr. Res.* **2022**, *511*, 108463, DOI 10.1016/j.carres.2021.108463.
[49] W. Guo, H. C. Bruining, H. J. Heeres, J. Yue, *Green Chem.* **2023**, *25*, 5878–5898.
[50] O. Ershova, J. Kanervo, S. Hellsten, H. Sixta, *RSC Adv.* **2015**, *5*, 66727–66737.
[51] J. Tuteja, S. Nishimura, K. Ebitani, *Bull. Chem. Soc. Jpn.* **2012**, *85*, 275–281.

[52] Y. Zhao, H. Xu, K. Lu, Y. Qu, L. Zhu, S. Wang, *Ind. Eng. Chem. Res.* **2019**, *58*, 17088–17097.
[53] A. Golon, N. Kuhnert, *Food Funct.* **2013**, *4*, 1040–1050.
[54] Q. Jing, X. Lü, *Chin. J. Chem. Eng.* **2008**, *16*, 890–894.
[55] Q. Jing, X. Lu, L. Yuan, *Huaxue Fanying Gongcheng Yu Gongyi/Chemical Reaction Engineering and Technology* **2006**, *22*, 472–475.
[56] Y. Yu, H. Wu, *Ind. Eng. Chem. Res.* **2011**, *50*, 10500–10508.
[57] M. Möller, F. Harnisch, U. Schröder, *Biomass Bioenergy* **2012**, *39*, 389–398.
[58] Z. Yan, J. Lian, Y. Feng, M. Li, F. Long, R. Cheng, S. Shi, H. Guo, J. Lu, *Fuel* **2021**, *289*, 119969.
[59] X. J. Chen, X. Q. Liu, F. L. Xu, X. P. Bai, *Adv Mat Res* **2012**, *450–451*, 710–714.
[60] E. R. Garrett, B. H. Dvorchik, *Kinetics and Mechanisms of the Acid Degradation of the Aldopentoses to Furfural* **1969**.
[61] K. Gairola, I. Smirnova, *Bioresour. Technol.* **2012**, *123*, 592–598.
[62] A. M. J. Kootstra, N. S. Mosier, E. L. Scott, H. H. Beeftink, J. P. M. Sanders, *Biochem. Eng. J.* **2009**, *43*, 92–97.
[63] J. M. R. Gallo, D. M. Alonso, M. A. Mellmer, J. H. Yeap, H. C. Wong, J. A. Dumesic, *Top. Catal.* **2013**, *56*, 1775–1781.
[64] J. Köchermann, J. Mühlenberg, M. Klemm, *Ind. Eng. Chem. Res.* **2018**, *57*, 14417–14427.
[65] Z. Chen, W. Zhang, J. Xu, P. Li, *Chin. J. Chem. Eng.* **2015**, *23*, 659–666.
[66] R. L. de Souza, H. Yu, F. Rataboul, N. Essayem, *Challenges* **2012**, *3*, 212–232.
[67] E. Domínguez, P. G. del Río, A. Romaní, G. Garrote, P. Gullón, A. de Vega, *Agronomy* **2020**, *10*, 1205, DOI 10.3390/agronomy10081205.
[68] L. Almhofer, R. H. Bischof, M. Madera, C. Paulik, *Can. J. Chem. Eng.* **2022**, *101*, 2033–2049, DOI 10.1002/cjce.24593.
[69] K. Lamminpää, J. Ahola, J. Tanskanen, *Ind. Eng. Chem. Res.* **2012**, *51*, 6297–6303.
[70] P. Körner, D. Jung, A. Kruse, *Green Chem.* **2018**, *20*, 2231–2241.
[71] S. Rok, M. Grilc, M. Hus, B. Likozar, *Ind. Eng. Chem. Res.* **2019**, DOI 10.1021/acs.iecr.9b00898.
[72] R. J. Van Putten, J. N. M. Soetedjo, E. A. Pidko, J. C. Van Der Waal, E. J. M. Hensen, E. De Jong, H. J. Heeres, *ChemSusChem* **2013**, *6*, 1681–1687.
[73] Y. Onishi, Y. Furushiro, Y. Hirayama, S. Adachi, T. Kobayashi, *Carbohydr. Res.* **2020**, *493*, 108031, DOI 10.1016/j.carres.2020.108031.
[74] S. Liu, Y. Zhu, Y. Liao, H. Wang, Q. Liu, L. Ma, C. Wang, *Applications in Energy and Combustion Science* **2022**, *10*, 100062, DOI 10.1016/j.jaecs.2022.100062.
[75] R. Weingarten, J. Cho, R. Xing, W. C. Conner, G. W. Huber, *ChemSusChem* **2012**, *5*, 1280–1290.
[76] B. Girisuta, L. P. B. M. Janssen, H. J. Heeres, *Green Chem.* **2006**, *8*, 701–709.
[77] N. T. Hoai, A. Sasaki, M. Sasaki, H. Kaga, T. Kakuchi, T. Satoh, *Carbohydr. Res.* **2011**, *346*, 1747–1751.
[78] C. Usuki, Y. Kimura, S. Adachi, *Food Sci. Technol. Res.* **2007**, *13*, 205–209.
[79] S. Liu, X. Cheng, S. Sun, Y. Chen, B. Bian, Y. Liu, L. Tong, H. Yu, Y. Ni, S. Yu, *ACS Omega* **2021**, *6*, 15940–15947.
[80] R. Ringgani, M. M. Azis, R. Rochmadi, A. Budiman, *Bulletin of Chemical Reaction Engineering and Catalysis* **2022**, *17*, 451–465.
[81] D. Y. Murzin, E. V. Murzina, A. Aho, M. A. Kazakova, A. G. Selyutin, D. Kubicka, V. L. Kuznetsov, I. L. Simakova, *Catal. Sci. Technol.* **2017**, *7*, 5321–5331.
[82] X. Hu, L. Wu, Y. Wang, Y. Song, D. Mourant, R. Gunawan, M. Gholizadeh, C. Z. Li, *Bioresour. Technol.* **2013**, *133*, 469–474.
[83] T. Dallas Swift, H. Nguyen, A. Anderko, V. Nikolakis, D. G. Vlachos, *Green Chem.* **2015**, *17*, 4725–4735.
[84] M. E. Toif, M. Hidayat, R. Rochmadi, A. Budiman, *Sugar Tech* **2023**, *25*, 234–244.
[85] J. B. Binder, A. V. Cefali, J. J. Blank, R. T. Raines, *Energy Environ. Sci.* **2010**, *3*, 765–771.
[86] H. S. Kim, G. T. Jeong, *Korean J. Chem. Eng.* **2018**, *35*, 2232–2240.
[87] S. Meier, *Catal. Sci. Technol.* **2020**, *10*, 1724–1730.
[88] T. Dallas Swift, H. Nguyen, A. Anderko, V. Nikolakis, D. G. Vlachos, *Green Chem.* **2015**, *17*, 4725–4735.
[89] K. Dussan, B. Girisuta, M. Lopes, J. J. Leahy, M. H. B. Hayes, *ChemSusChem* **2016**, *9*, 492–504.

Manuscript received: May 5, 2024
Revised manuscript received: June 25, 2024
Accepted manuscript online: July 3, 2024
Version of record online: September 3, 2024